



CrossMark
 click for updates

Cite this: *RSC Adv.*, 2015, 5, 37675

Nb-doped VO_x/CeO₂ catalyst for NH₃-SCR of NO_x at low temperatures†

Zhihua Lian, Fudong Liu,‡* Hong He* and Kuo Liu

The promotion effect of Nb addition to VO_x/CeO₂ catalysts for the selective catalytic reduction of NO_x by NH₃ was fully investigated. VO_x/CeO₂ and NbO_x doped VO_x/CeO₂ catalysts were characterized by N₂ physisorption, XRD, H₂-TPR and NH₃-TPD. The results showed that the addition of Nb could significantly promote the SCR activity of the VO_x/CeO₂ catalyst, especially in the low temperature range. VO_x/CeO₂ with 30 wt% NbO_x catalyst showed the best catalytic performance and better SO₂/H₂O tolerance than VO_x/CeO₂ catalyst. 30Nb-1VO_x/CeO₂ also exhibited higher NH₃-SCR activity than 3V₂O₅-WO₃/TiO₂. Lower crystallinity, stronger redox capability and more Brønsted acid sites of the Nb-VO_x/CeO₂ catalyst were all responsible for its more excellent NH₃-SCR performance. Based on kinetic experiments and *in situ* DRIFTS results, it was concluded that the Langmuir–Hinshelwood mechanism existed for selective catalytic reduction of NO over Nb-VO_x/CeO₂, in which adsorbed NO_x species reacted with adsorbed NH₃ to finally form N₂ and H₂O.

Received 12th February 2015
 Accepted 20th April 2015

DOI: 10.1039/c5ra02752g

www.rsc.org/advances

1 Introduction

Nitrogen oxides (NO and NO₂), which result from automobile exhaust gas and industrial combustion of fossil fuels, are major air pollutants.¹ They contribute to a variety of environmentally harmful effects such as photochemical smog, acid rain, and haze formation.² The selective catalytic reduction of NO_x with NH₃ (NH₃-SCR) in the presence of excess oxygen is now the most efficient technology for the removal of nitrogen oxides from stationary sources.^{2,3} V₂O₅-WO₃(MoO₃)/TiO₂ has been widely applied as an industrial catalyst for several decades.^{4,5} However, some problems still remain for V₂O₅-WO₃(MoO₃)/TiO₂, such as the relatively narrow operating temperature window of 300–400 °C, low N₂ selectivity and high conversion of SO₂ to SO₃ at high temperatures.^{4,6,7} Besides, the high concentration of ash containing K₂O, CaO, As₂O₃ in the flue gas reduces the performance and longevity of V₂O₅-WO₃(MoO₃)/TiO₂ catalysts.^{8,9} These could be avoided by locating the SCR unit downstream of the electrostatic precipitator unit and even downstream of the desulfurizer, through the development of a highly efficient low temperature SCR system.

In our previous study, we have developed a VO_x/CeO₂ catalyst, prepared by a homogeneous precipitation method, showing excellent NH₃-SCR activity, N₂ selectivity and SO₂

durability.¹⁰ However, the catalytic activity was not high enough for the application in the deNO_x process of exhaust gas with low temperature, such as the flue gas after dust removal and desulfurization from coal-fired power plants. Therefore, it is very necessary to modify this vanadium–cerium catalyst to improve the low temperature activity, which is crucial for its practical utilization.

Niobium compound materials are of current interest as important catalysts for various reactions, such as the removal of nitrogen oxides, the hydrogenation and oxidative dehydrogenation of alkanes, acting as a catalyst promoter, catalyst support or solid acid catalyst.¹¹ It was reported that when the niobium oxides were introduced into V₂O₅/TiO₂ catalysts, the conversion of NO in NH₃-SCR reaction increased 2–4 times at low temperatures.¹² The addition of Nb to MnO_x-CeO₂ was also found to be very effective in improving the NH₃-SCR activity and N₂ selectivity.^{13,14} Mn₂Nb₁O_x catalyst exhibited higher NH₃-SCR activity than MnO_x catalyst.¹⁵ In addition, it was reported that the introduction of the third main group element (such as Mn, Fe, Co, Mo) could also improve the activity, stability or SO₂ durability of the SCR catalysts.^{16–19} Therefore, based on our V–Ce catalyst, we can add other elements to adjust its physicochemical properties, expecting to enhance the low temperature SCR activity.

In this study, a series of M-VO_x/CeO₂ catalysts (M = Mn, Fe, Co, Nb, Mo) were prepared by the homogeneous precipitation method and were applied to the low-temperature NH₃-SCR reaction. The addition of Nb could significantly promote the SCR activity over the VO_x/CeO₂ catalyst. Among the catalysts with different NbO_x contents, VO_x/CeO₂ with 30 wt% NbO_x catalyst showed the best catalytic performance and better SO₂/H₂O tolerance compared to VO_x/CeO₂ catalyst. The lower

State Key Joint Laboratory of Environment Simulation and Pollution Control, Research Center for Eco-Environmental Sciences, Chinese Academy of Sciences, Beijing 100085, PR China. E-mail: fudongliu@lbc.gov; lfd1982@gmail.com; honghe@rcees.ac.cn; Fax: +86 10 62849123; Tel: +86 10 62849123

† Electronic supplementary information (ESI) available. See DOI: 10.1039/c5ra02752g

‡ Present address: Materials Sciences Division, Lawrence Berkeley National Laboratory, 1 Cyclotron Road, Berkeley, CA 94720, USA.

crystallinity, the stronger redox capability and the more Brønsted acid sites of the Nb-VO_x/CeO₂ catalyst were all responsible for its higher SCR activity.

2 Experiments

2.1 Catalyst synthesis and activity tests

The VO_x/CeO₂ oxide catalysts were prepared by a homogeneous precipitation method. Aqueous solutions of NH₄VO₃ (H₂C₂O₄ was added to facilitate the dissolution of NH₄VO₃) and Ce(NO₃)₂ were mixed with the desired molar ratios (the mass ratio of vanadium oxide was controlled at 1 wt%). An excess of aqueous urea solution was then added to the mixed solution. The solution was heated to 90 °C and held there for 12 h under vigorous stirring. After filtration and washing with deionized water, the resulting precipitate was dried at 100 °C overnight and subsequently calcined at 350 °C for 3 h in air. M-VO_x/CeO₂ catalysts (the mass ratio of MO_x were controlled at 30 wt%) were also prepared by homogeneous precipitation methods using Mn(NO₃)₂, Co(NO₃)₃, Fe(NO₃)₃, NbCl₅, and (NH₄)₆Mo₇O₂₄ as precursors, respectively. Nb-VO_x/CeO₂ catalysts with different Nb contents (10, 30, 50 wt%) and the unpromoted 3 wt% VO_x/CeO₂ catalyst were also prepared by the same method. For comparison, the conventional 3 wt% V₂O₅-10 wt% WO₃/TiO₂ and 1 wt% V₂O₅-10 wt% WO₃/TiO₂ were prepared by impregnation method using NH₄VO₃, (NH₄)₁₀W₁₂O₄₁ as precursors and anatase TiO₂ as support. After impregnation, the excess water was removed in a rotary evaporator at 60 °C. The samples dried at 100 °C overnight and then calcined at 500 °C for 3 h in air condition.

Before NH₃-SCR activity tests, the catalysts were pressed, crushed and sieved to 40–60 mesh. The SCR activity tests were carried out in a fixed-bed quartz flow reactor at atmospheric pressure. The reaction conditions were controlled as follows: 500 ppm NO, 500 ppm NH₃, 5 vol% O₂, 100 ppm SO₂ (when used), 5 vol% H₂O (when used), N₂ balance. Under ambient conditions, the total flow rate was 500 ml min⁻¹ and the gas hourly space velocity (GHSV) was 50 000 h⁻¹. The amount of catalysts used in activity tests was 0.6 ml (about 0.7 g). The effluent gas including NO, NH₃, NO₂ and N₂O was continuously analyzed by an FTIR spectrometer (Nicolet Nexus 670) equipped with a heated, low-volume multiple-path gas cell (2m). The FTIR spectra were collected after the SCR reaction reached a steady state, and the NO_x conversion and N₂ selectivity were calculated as follows:

$$\text{NO}_x \text{ conversion} = \left(1 - \frac{[\text{NO}]_{\text{out}} + [\text{NO}_2]_{\text{out}}}{[\text{NO}]_{\text{in}} + [\text{NO}_2]_{\text{in}}} \right) \times 100\%$$

$$\text{N}_2 \text{ selectivity} = \frac{[\text{NO}]_{\text{in}} + [\text{NH}_3]_{\text{in}} - [\text{NO}_2]_{\text{out}} - 2[\text{N}_2\text{O}]_{\text{out}}}{[\text{NO}]_{\text{in}} + [\text{NH}_3]_{\text{in}}} \times 100\%$$

2.2 Characterization of catalysts

The surface area and pore characterization of the catalysts were obtained from N₂ adsorption/desorption analysis at -196 °C using a Quantachrome Quadrasorb SI-MP. Prior to the N₂

physisorption, the catalysts were degassed at 300 °C for 5 h. Surface areas were determined by the BET equation in the 0.05–0.35 partial pressure range. Pore volumes and average pore diameters were determined by the Barrett–Joyner–Halenda (BJH) method from the desorption branches of the isotherms.

Powder X-ray diffraction (XRD) measurements of the catalysts were carried out on a computerized PANalytical X'Pert Pro diffractometer with Cu Kα (λ = 0.15406 nm) radiation. The data of 2θ from 10 to 80° were collected at 8° min⁻¹ with the step size of 0.07°.

The H₂-TPR experiments were carried out on a Micromeritics Auto Chem 2920 chemisorption analyzer. The samples (30 mg) were pretreated at 300 °C in a flow of 20 vol% O₂/Ar (50 ml min⁻¹) for 0.5 h in a quartz reactor and cooled down to room temperature (30 °C) followed by Ar purging for 0.5 h. A 50 ml min⁻¹ gas flow of 10% H₂ in Ar was then passed over the samples through a cold trap to the detector. The reduction temperature was raised at 10 °C min⁻¹ from 30 to 1000 °C.

2.3 NH₃-TPD studies

NH₃-TPD experiments were performed in the same instrument as the H₂-TPR, equipped with a quadrupole mass spectrometer (MKS Cirrus) to record the signals of NH₃ (m/z = 17 for NH₃, the interference of H₂O was eliminated by using a cold trap before the detector). Prior to TPD experiments, the samples (100 mg) were pretreated at 300 °C in a flow of 20 vol% O₂/Ar (50 ml min⁻¹) for 0.5 h and cooled down to room temperature (30 °C). The samples were then exposed to a flow of 2500 ppm NH₃/Ar (50 ml min⁻¹) at 30 °C for 1 h, followed by Ar purging for another 1 h. Finally, the temperature was raised to 600 °C in Ar flow at the rate of 10 °C min⁻¹.

2.4 In situ DRIFTS studies

In situ DRIFTS experiments were performed on an FTIR spectrometer (Nicolet Nexus 670) equipped with a smart collector and an MCT/A detector cooled by liquid nitrogen. The reaction temperature was controlled precisely by an Omega programmable temperature controller. Prior to each experiment, the sample was pretreated at 300 °C for 0.5 h in a flow of 20 vol% O₂/N₂ and then cooled down to 175 °C. The background spectra were collected in flowing N₂ and automatically subtracted from the sample spectrum. The reaction conditions were controlled as follows: 200 ml min⁻¹ total flow rate, 500 ppm NH₃ or/and 500 ppm NO + 5 vol% O₂, and N₂ balance. All spectra were recorded by accumulating 100 scans with a resolution of 4 cm⁻¹.

3 Results and discussion

3.1 Catalytic performance

3.1.1 SCR activity over 30M-1VO_x/CeO₂. Fig. 1 shows the NO_x conversion and N₂ selectivity over VO_x/CeO₂ and doped VO_x/CeO₂ catalysts. The VO_x/CeO₂ catalyst presented 80% NO_x conversion at 200 °C. Mn doped VO_x/CeO₂ exhibited nearly 100% NO_x conversion at 100–200 °C, but the NO_x conversion decreased rapidly above 200 °C. It also showed lower N₂ selectivity in the whole temperature that we investigated. NH₃-SCR

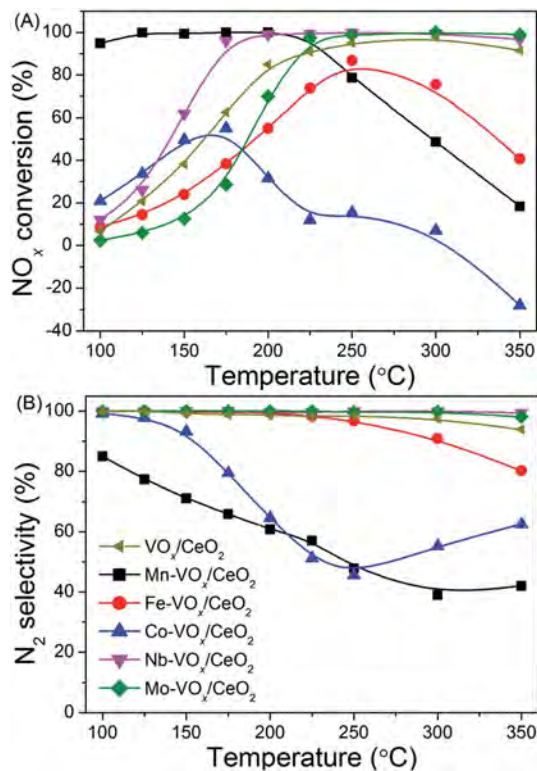


Fig. 1 The NO_x conversion (A) and N_2 selectivity (B) over M- VO_x/CeO_2 catalysts. Reaction conditions: $[\text{NO}] = [\text{NH}_3] = 500$ ppm, $[\text{O}_2] = 5$ vol%, N_2 balance, total flow rate 500 ml min^{-1} and GHSV = $50\,000 \text{ h}^{-1}$.

activities over Fe, Co and Mo doped VO_x/CeO_2 catalysts were all lower than that over VO_x/CeO_2 . Among these catalysts, Co doped VO_x/CeO_2 catalyst presented the lowest NO_x conversion and the maximal NO_x conversion was only 50%. Furthermore, the N_2 selectivity over Co- VO_x/CeO_2 was rather low. Contrarily, Nb doped VO_x/CeO_2 catalyst exhibited higher catalytic performance than the VO_x/CeO_2 catalyst. The addition of Nb enhanced the NO_x conversion and N_2 selectivity over VO_x/CeO_2 simultaneously. It showed 60% and 90% NO_x conversion at 150 and 175 °C, respectively, and 100% N_2 selectivity was obtained in the temperature range of 100–350 °C. The best NH_3 -SCR activity was obtained over the Nb doped VO_x/CeO_2 catalyst, therefore we chose Nb to further investigate the influence of doping amount on the catalyst structure and catalytic performance.

3.1.2 SCR activity over Nb-1 VO_x/CeO_2 catalysts. The effect of NbO_x addition amount to VO_x/CeO_2 catalyst on NO_x conversion was shown in Fig. 2. 10 wt% NbO_x doped VO_x/CeO_2 catalyst showed higher NH_3 -SCR activity than unpromoted VO_x/CeO_2 catalyst. The 30Nb- VO_x/CeO_2 catalyst presented the best catalytic activity, over which NO_x was completely reduced at about 175 °C. Any further increase in Nb content resulted in a decline in activity. These indicated that Nb content had a significant effect on the SCR activity over VO_x/CeO_2 catalysts, and 30 wt% NbO_x was optimal. Although, for the 30Nb- VO_x/CeO_2 catalyst, the content of 1% V seems to be negligible comparing with 30% Nb, V indeed played an important role in NH_3 -SCR reaction and 30Nb- VO_x/CeO_2 exhibited much higher catalytic activity than

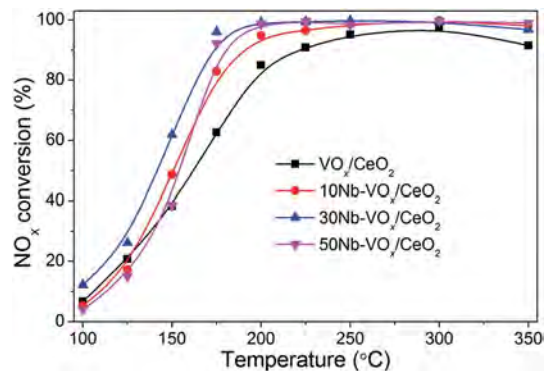


Fig. 2 NH_3 -SCR activity over Nb- VO_x/CeO_2 catalysts. Reaction conditions: $[\text{NO}] = [\text{NH}_3] = 500$ ppm, $[\text{O}_2] = 5$ vol%, N_2 balance, total flow rate 500 ml min^{-1} and GHSV = $50\,000 \text{ h}^{-1}$.

30Nb/ CeO_2 (as shown in Fig. S1†). At lower than 175 °C, the reaction rates normalized by surface area over 30Nb- VO_x/CeO_2 was higher than that over VO_x/CeO_2 (as shown in Fig. S2†). The highest reaction rate over 30Nb- VO_x/CeO_2 was obtained at 175–350 °C. The lower reaction rates over 30Nb- VO_x/CeO_2 than VO_x/CeO_2 above 200 °C were due to its larger specific surface area and similar NO_x conversion. 30Nb-1 VO_x/CeO_2 and 1 VO_x/CeO_2 catalyst were chosen as the model catalysts to carry out further investigation, such as the effect of Nb on $\text{H}_2\text{O}/\text{SO}_2$ tolerance and the relationship between catalyst structure and catalytic activity.

To better evaluate the NH_3 -SCR activity over Nb- VO_x/CeO_2 catalyst, we also carried out the comparative SCR activity test over $\text{V}_2\text{O}_5\text{-WO}_3/\text{TiO}_2$ (Fig. 3). 30 wt% Nb-1 VO_x/CeO_2 exhibited higher NO_x conversion than 1 VO_x/CeO_2 and 3 VO_x/CeO_2 . However, there was not notable enhancement over 30Nb-3 VO_x/CeO_2 in contrast to 3 VO_x/CeO_2 (as shown in Fig. S3†). Compared to 3 VO_x/CeO_2 , the 30Nb-1 VO_x/CeO_2 catalyst not only decreased the content of vanadium oxide, but also enhanced the catalytic activity. The NH_3 -SCR performance over 30Nb-1 VO_x/CeO_2 catalyst was also better than that over 3 $\text{V}_2\text{O}_5\text{-10WO}_3/\text{TiO}_2$ and 1 $\text{V}_2\text{O}_5\text{-10WO}_3/\text{TiO}_2$. The NO_x conversion over three catalysts at 175 °C was 96%,

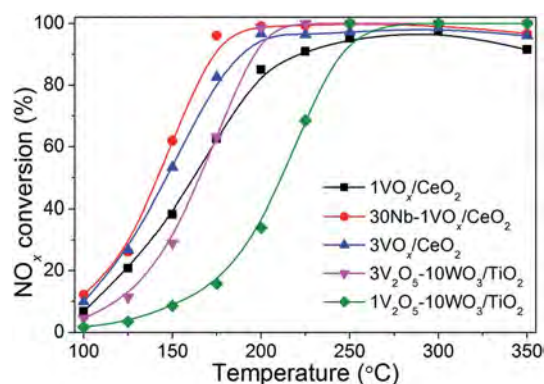


Fig. 3 NH_3 -SCR activity over VO_x/CeO_2 and $\text{V}_2\text{O}_5\text{-WO}_3/\text{TiO}_2$ catalysts. Reaction conditions: $[\text{NO}] = [\text{NH}_3] = 500$ ppm, $[\text{O}_2] = 5$ vol%, N_2 balance, total flow rate 500 ml min^{-1} and GHSV = $50\,000 \text{ h}^{-1}$.

63% and 15%, respectively. Therefore, 30Nb-1VO_x/CeO₂ showed excellent NH₃-SCR performance.

3.1.3 Influence of H₂O and SO₂ on SCR activity. Fig. 4 shows the effect of SO₂ and H₂O on the catalytic activity over 1VO_x/CeO₂ and 30Nb-1VO_x/CeO₂ catalysts at 250 °C. When 100 ppm SO₂ was introduced to the inlet gas, the NO_x conversion over VO_x/CeO₂ decreased to 24% in 48 h and could not recover to the initial activity after the removal of SO₂, which indicates that the inhibiting effect of SO₂ on the SCR activity over the VO_x/CeO₂ catalyst was severe and irreversible. However, the SO₂ inhibiting effect over Nb-VO_x/CeO₂ was quite different. The NO_x conversion decreased slightly, and nearly 90% NO_x conversion was obtained in the presence of 100 ppm SO₂ for a 48 h test. The NH₃-SCR performance over VO_x/CeO₂ catalysts after SO₂ poisoning for 48 h is shown in Fig. S4.† The activity over sulfated-Nb-VO_x/CeO₂ was still higher than that over sulfated-VO_x/CeO₂. 95% NO_x conversion could be obtained on the sulfated-Nb-VO_x/CeO₂ catalyst at 250 °C and only 26% NO_x conversion on sulfated-VO_x/CeO₂. This proved again that the Nb-VO_x/CeO₂ catalyst showed higher SO₂ resistance than VO_x/CeO₂.

When 5% H₂O was introduced to the inlet gas, the NO_x conversion over VO_x/CeO₂ decreased rapidly to 56% and kept in 56% in 48 h test. The catalytic activity could recover to the original level after the removal of H₂O, indicating that the poison of H₂O was reversible. Meanwhile, H₂O had no influence on the catalytic activity over Nb-VO_x/CeO₂ catalyst and 100% NO_x conversion was maintained all the time. Nb-VO_x/CeO₂ exhibited much higher catalytic activity and stronger resistance to SO₂/H₂O than VO_x/CeO₂.

3.2 Catalyst characterization

3.2.1 N₂ physisorption. Table 1 shows the N₂ physisorption results of 1VO_x/CeO₂ and 30Nb-1VO_x/CeO₂ catalysts. Nb-VO_x/CeO₂ catalyst presented larger specific surface area and pore volume than VO_x/CeO₂. The addition of Nb to VO_x/CeO₂

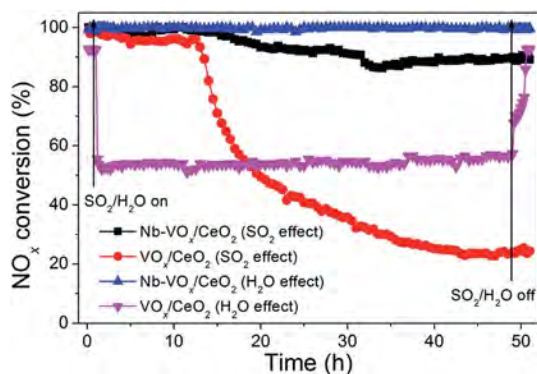


Fig. 4 Effect of SO₂ and H₂O on NH₃-SCR activity over VO_x/CeO₂ and Nb-VO_x/CeO₂ catalysts at 250 °C. Reaction conditions: [NO] = [NH₃] = 500 ppm, [SO₂] = 100 ppm (when used), [H₂O] = 5 vol% (when used), [O₂] = 5 vol%, N₂ balance, total flow rate 500 ml min⁻¹ and GHSV = 50 000 h⁻¹.

Table 1 N₂ physisorption of VO_x/CeO₂ and Nb-VO_x/CeO₂ catalysts

Catalysts	Specific surface area (m ² g ⁻¹)	Pore diameter (nm)	Pore volume (cm ⁻³ g ⁻¹)
1VO _x /CeO ₂	131.3	3.50	0.11
30Nb-1VO _x /CeO ₂	168.2	3.48	0.15

resulted in bigger specific surface area and pore volume, which is beneficial to the enhancement of SCR activity.

3.2.2 XRD. The XRD patterns of 1VO_x/CeO₂ and 30Nb-1VO_x/CeO₂ catalysts are shown in Fig. 5. For both catalysts, all the peaks in the diffraction profiles attributed to CeO₂ of a cubic fluorite structure (43-1002). No vanadium species and niobium species were detected, suggesting that V and Nb species were highly dispersed on the catalysts. The intensity of peaks of Nb doped catalyst was weaker than that of VO_x/CeO₂, indicating a loss of crystallinity. The decreasing crystallinity may contribute to the increase of surface area.

3.2.3 H₂-TPR. The redox properties of 1VO_x/CeO₂ and 30Nb-1VO_x/CeO₂ catalysts were investigated by H₂-TPR and the spectra are shown in Fig. 6. There are three peaks at 380, 460 and 710 °C (740 °C) over 1VO_x/CeO₂ and 30Nb-1VO_x/CeO₂. According to the literatures,^{10,20} the reduction peaks of surface Ce⁴⁺ to Ce³⁺ and the bulk Ce⁴⁺ to Ce³⁺ were centered at 509 and 812 °C, respectively. The reduction peaks at 399, 523 and 766 °C over CeO₂ could be assigned to the reduction of surface oxygen species, that of oxygen in deeper interior and that of oxygen in bulk, respectively.²¹ The reduction peak around 400–500 °C is due to the surface vanadium oxide, while high temperature peak over 700 °C is assigned to the reduction of bulk vanadium oxide.²² Niobium oxide could be reduced at much higher temperature.¹⁵ Therefore, the low temperature peak at 380 °C and 460 °C could be due to the reduction of surface Ce⁴⁺ and V⁵⁺ and that in deeper interior, respectively. The TPR peak at 710 °C (740 °C) could be attributed to the reduction of bulk Ce and V. Both V and Ce possessed redox capability and acted as reactive sites to catalyze NH₃-SCR reaction. The amount of H₂ consumption of Nb-VO_x/CeO₂ catalyst was higher than that of VO_x/CeO₂ (1.15 : 1). The intensity of the low temperature (380 °C) reduction peak of Nb-VO_x/CeO₂ was much stronger

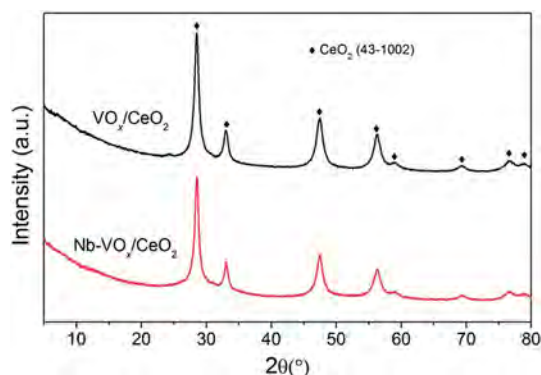


Fig. 5 XRD patterns of VO_x/CeO₂ and Nb-VO_x/CeO₂ catalysts.

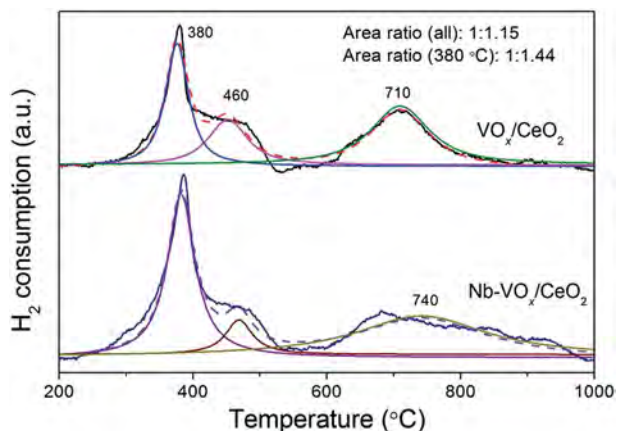


Fig. 6 H₂-TPR results over VO_x/CeO₂ and Nb-VO_x/CeO₂ catalysts.

than that of VO_x/CeO₂ (1.44 : 1). This could be due to the interaction of V, Ce and Nb over Nb-VO_x/CeO₂ catalyst resulting in better dispersion of vanadium species and stronger redox capability. The active temperature window in NH₃-SCR reaction was between 150–400 °C. Stronger redox capability in this temperature range could enhance NH₃-SCR performance. Therefore, Nb doped VO_x/CeO₂ showed higher NH₃-SCR activity.

3.3 NH₃-TPD

Fig. 7 shows NH₃-TPD results over 1VO_x/CeO₂ and 30Nb-1VO_x/CeO₂ catalysts using the fragment of $m/z = 17$ to identify NH₃. There were two NH₃ desorption peaks around 100 and 250 °C on both catalysts. It is generally accepted that NH₄⁺ ions bound to Brønsted acid sites are less thermally stable than coordinated NH₃ molecules bound to Lewis acid sites and desorb at lower temperatures.^{18,23,24} Therefore, the desorption peak at 100 °C could be ascribed to the desorption of physisorbed NH₃ and the partial ionic NH₄⁺ bound to the weak Brønsted acid sites, and the peak at 250 °C could be assigned to the desorption of ionic NH₄⁺ bound to strong Brønsted acid sites and coordinated NH₃ bound to the Lewis acid sites. The amount of acid sites over Nb-VO_x/CeO₂ was remarkably larger than that of VO_x/CeO₂ (1.68 : 1). It indicates that Nb-VO_x/CeO₂ catalyst presented more acid sites which could facilitate the

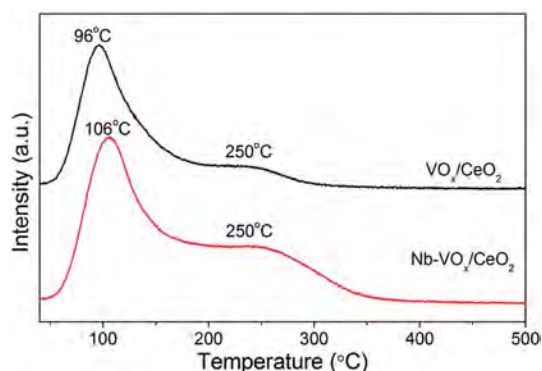


Fig. 7 NH₃-TPD results over VO_x/CeO₂ and Nb-VO_x/CeO₂ catalysts.

adsorption and activation of NH₃ during catalytic reaction even in the presence of H₂O and SO₂ thus enhances the catalytic activity in NH₃-SCR. In the presence of SO₂, more acid sites over Nb-VO_x/CeO₂ catalyst inhibited the adsorption of SO₂ and the deposition of sulfate thus enhanced the resistance to SO₂. More acid sites could also promote the adsorption of NH₃ in the presence of H₂O and reduce the influence of competitive adsorption of H₂O with NH₃. Furthermore, larger specific surface area was obtained over Nb-VO_x/CeO₂. Therefore, Nb-VO_x/CeO₂ catalyst showed stronger resistance to H₂O/SO₂.

3.4 In situ DRIFTS studies

To investigate NH₃/NO_x adsorption on 1VO_x/CeO₂ and 30Nb-1VO_x/CeO₂ catalysts together with the SCR reaction mechanism, *in situ* DRIFTS were conducted at 175 °C and the results of NH₃ adsorption on VO_x/CeO₂ and Nb-VO_x/CeO₂ catalysts are shown in Fig. 8A. After NH₃ adsorption and N₂ purge, both catalysts were covered by different NH₃ species. The bands at 1423 and 1670 cm⁻¹ were assigned to asymmetric and symmetric bending vibrations of ionic NH₄⁺ on Brønsted acid sites and the bands at 1596 (1604) and 1147 (1200) cm⁻¹ were attributed to asymmetric and symmetric bending vibrations of the N–H bonds in NH₃ coordinately linked to the Lewis acid sites.^{25–27} Nb-VO_x/CeO₂ catalyst provided more acid sites than VO_x/CeO₂ (1.71 : 1), especially the Brønsted acid sites, than VO_x/CeO₂, which was in well harmony with the NH₃-TPD results. As shown in our previous paper (*Chem. Eng. J.*, 2014, 250, 390–398),¹⁵ the NbO_x itself did not show any NH₃-SCR activity in the whole temperature range that we investigated. However, the addition of Nb to 1VO_x/CeO₂ increased the surface acidity. Nb mainly played as acid sites for the promotion of NH₃ adsorption in NH₃-SCR reaction.

The *in situ* DRIFT spectra of NO + O₂ adsorption on 1VO_x/CeO₂ and 30Nb-1VO_x/CeO₂ catalysts at 175 °C were also conducted, and the results are shown in Fig. 8B. When VO_x/CeO₂ catalyst was exposed to NO + O₂, bands assigned to nitrate species were observed including monodentate nitrate (1540 and 1270 cm⁻¹), bridging nitrate (1215 and 1592 cm⁻¹) and bidentate nitrate (1570 and 1243 cm⁻¹).^{28–30} On the Nb-VO_x/CeO₂ catalyst, the

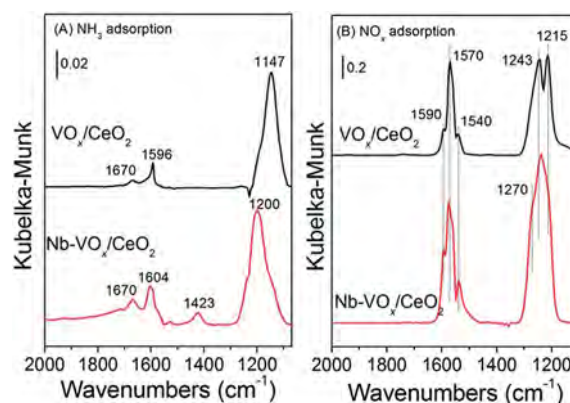


Fig. 8 DRIFT spectra of 500 ppm NH₃ adsorption (A) and 500 ppm NO + 5 vol% O₂ adsorption (B) on VO_x/CeO₂ and Nb-VO_x/CeO₂ catalysts.

adsorption amount of NO_x was larger than that on the VO_x/CeO_2 catalyst (1.67 : 1). The addition of Nb to the VO_x/CeO_2 catalyst increased the acidity but did not inhibit the adsorption of NO_x on the catalyst surface simultaneously. It could be due to its stronger oxidation at low temperature and its larger specific surface area. Therefore, the $\text{Nb-VO}_x/\text{CeO}_2$ catalyst produced more nitrate species than VO_x/CeO_2 .

According to the Arrhenius equation, the activation energy over VO_x/CeO_2 and $\text{Nb-VO}_x/\text{CeO}_2$ catalysts was calculated as 47 and 38 kJ mol^{-1} (as shown in Fig. S5†). The interaction of V, Ce and Nb of the $\text{Nb-VO}_x/\text{CeO}_2$ catalyst decreased the activation energy of NO reduction and promote the NH_3 -SCR reaction.

To investigate the reactivity of adsorbed NH_3 species in the SCR reaction on $30\text{Nb-1VO}_x/\text{CeO}_2$ catalysts, the *in situ* DRIFTS of reaction between pre-adsorbed NH_3 and $\text{NO} + \text{O}_2$ at 175°C were recorded as a function of time (Fig. 9A). After NH_3 pre-adsorption and N_2 purge, the catalyst surface was covered by the adsorbed NH_3 species. When $\text{NO} + \text{O}_2$ was introduced, the intensity of the bands attributed to NH_3 species decreased and disappeared after 10 min. At the same time, the bands assigned to nitrate species (monodentate nitrate at 1540 cm^{-1} , bridging nitrate at $1215, 1592\text{ cm}^{-1}$ and bidentate nitrate at $1570, 1243\text{ cm}^{-1}$) appeared. This result suggested that both ionic NH_4^+ and coordinated NH_3 could react with NO_x and participate in the NH_3 -SCR reactions. Fig. S6† showed the band intensities of adsorbed NH_3 species over VO_x/CeO_2 and $30\text{Nb-VO}_x/\text{CeO}_2$ pretreated by exposure to NH_3 followed by exposure to $\text{NO} + \text{O}_2$ at 175°C . The reactive rate of adsorbed NH_3 species with gas NO and O_2 over $\text{Nb-VO}_x/\text{CeO}_2$ was much higher than that over VO_x/CeO_2 . Therefore, more adsorbed NH_3 species on $\text{Nb-VO}_x/\text{CeO}_2$ contributed to its better SCR activity.

The reaction between the pre-adsorbed NO_x and NH_3 on $30\text{Nb-1VO}_x/\text{CeO}_2$ catalysts was also investigated by the *in situ* DRIFTS, and the results were shown in Fig. 9B. After $\text{NO} + \text{O}_2$ pre-adsorption and N_2 purge, $\text{Nb-VO}_x/\text{CeO}_2$ catalyst surface was covered by various nitrate species. When NH_3 was introduced, the intensity of bridging nitrate decreased, which indicated that adsorbed NO_x species could also react with NH_3 . NH_3 adsorbed species were observed at the band of 1427 cm^{-1} .

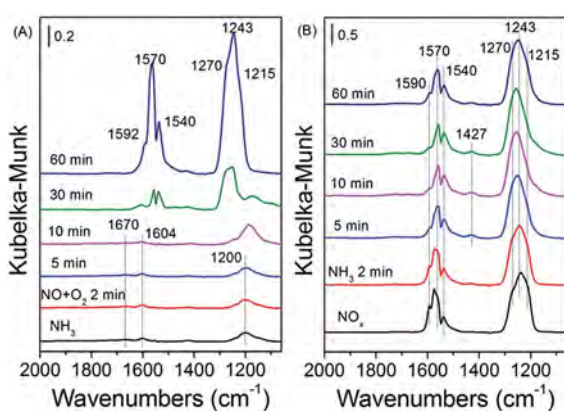


Fig. 9 *In situ* DRIFT spectra over $\text{Nb-VO}_x/\text{CeO}_2$ pretreated by exposure to $\text{NO} + \text{O}_2$ followed by exposure to NH_3 at 175°C (A), and by exposure to NH_3 followed by exposure to $\text{NO} + \text{O}_2$ at 175°C (B).

The kinetic experiments were also carried out to investigate the reaction order and the tests met the condition of differential reactor model. The NO conversion data in the kinetics test were in differential regime (conversion less than 20%) (as shown in Fig. S7†). A relative small particles size (40–60 mesh) and the volume hourly space velocity (about $500\,000\text{ h}^{-1}$)³¹ ensured the elimination of internal and external diffusion, respectively. The rates of NO conversion increased linearly with NO concentration over $30\text{Nb-1VO}_x/\text{CeO}_2$ catalyst (as shown in Fig. S8†), and the reaction order for NO was calculated as 0.555. The reaction order for NO was lower than 1, indicating the presence of Langmuir–Hinshelwood mechanism, which was in agreement with DRIFTS results. In Fig. 9B, the intensity of the bands attributed to nitrate species weakened after exposure to NH_3 , indicating that adsorbed NO_x species could react with adsorbed NH_3 to finally form N_2 and H_2O . In our previous study,¹⁰ for the $3\text{VO}_x/\text{CeO}_2$ catalysts pre-adsorbed NO_x species, when NH_3 was introduced, the intensity of the bands attributed to monodentate nitrate and bridging nitrate species decreased slightly. The amount of bidentate nitrate species increased markedly, which may be due to the transformation of monodentate and bridging nitrate to bidentate nitrate (Fig. 10 (ref. 10) and S5†¹⁰). The adsorbed nitrate species were mostly inactive in the NH_3 -SCR reaction and therefore the $3\text{VO}_x/\text{CeO}_2$ catalysts mainly followed the Eley–Rideal mechanism.

4 Conclusions

A systematic study on the effect of Nb addition to the VO_x/CeO_2 catalyst for the low-temperature NH_3 -SCR reaction was carried out. VO_x/CeO_2 and Nb doped VO_x/CeO_2 catalysts were prepared by homogeneous precipitation method and the SCR activity at low temperature was enhanced by the addition of Nb. The NH_3 -SCR activity over $1\%\text{VO}_x/\text{CeO}_2$ with 30 wt% NbO_x catalyst were higher than that over the $3\%\text{V}_2\text{O}_5\text{-WO}_3/\text{TiO}_2$ catalyst. $30\text{Nb-1VO}_x/\text{CeO}_2$ showed higher catalytic activity than $1\text{VO}_x/\text{CeO}_2$ catalyst, due to the weaker crystallinity, the stronger redox capability and the more Brønsted acid sites. The excellent $\text{SO}_2/\text{H}_2\text{O}$ tolerance was also obtained over $30\text{Nb-1VO}_x/\text{CeO}_2$ catalyst. The Langmuir–Hinshelwood mechanism existed for selective catalytic reduction of NO over $30\text{Nb-1VO}_x/\text{CeO}_2$, in which adsorbed NO_x species reacted with adsorbed NH_3 to finally form N_2 and H_2O .

Acknowledgements

This work was financially supported by the National Natural Science Foundation of China (51221892) and the Ministry of Science and Technology, China (2013AA065301).

References

- 1 G. S. Qi, R. T. Yang and R. Chang, *Appl. Catal., B*, 2004, **51**, 93.
- 2 H. Bosch and F. Janssen, *Catal. Today*, 1988, **2**, 369.
- 3 Z. G. Huang, Z. P. Zhu, Z. Y. Liu and Q. Y. Liu, *J. Catal.*, 2003, **214**, 213.
- 4 G. Busca, L. Lietti, G. Ramis and F. Berti, *Appl. Catal., B*, 1998, **18**, 1.

- 5 G. Busca, M. A. Larrubia, L. Arrighi and G. Ramis, *Catal. Today*, 2005, **107–108**, 139.
- 6 J. P. Dunn, P. R. Koppula, H. G. Stenger and I. E. Wachs, *Appl. Catal., B*, 1998, **19**, 103.
- 7 P. Balle, B. Geiger and S. Kureti, *Appl. Catal., B*, 2009, **85**, 109.
- 8 I. E. Wachs and B. M. Weckhuysen, *Appl. Catal., A*, 1997, **157**, 67.
- 9 D. A. Bulushev, F. Rainone, L. Kiwi-Minsker and A. Renken, *Langmuir*, 2001, **17**, 5276.
- 10 Z. Lian, F. Liu and H. He, *Catal. Sci. Technol.*, 2015, **5**, 389.
- 11 K. Tanabe, *Catal. Today*, 2003, **78**, 65.
- 12 K. A. Vikulov, A. Andreini, E. K. Poels and A. Bliet, *Catal. Lett.*, 1994, **25**, 49.
- 13 M. Casapu, O. Krocher, M. Mehring, M. Nachtegaal, C. Borca, M. Harfouche and D. Grolimund, *J. Phys. Chem. C*, 2010, **114**, 9791.
- 14 M. Casapu, O. Kröcher and M. Elsener, *Appl. Catal., B*, 2009, **88**, 413.
- 15 Z. Lian, F. Liu, H. He, X. Shi, J. Mo and Z. Wu, *Chem. Eng. J.*, 2014, **250**, 390.
- 16 F. Liu, H. He, Y. Ding and C. Zhang, *Appl. Catal., B*, 2009, **93**, 194.
- 17 X. Li and Y. Li, *J. Mol. Catal. A: Chem.*, 2014, **386**, 69.
- 18 S. Roy, B. Viswanath, M. S. Hedge and G. Madras, *J. Phys. Chem. C*, 2008, **112**, 6002.
- 19 Z. Liu, S. Zhang, J. Li and L. Ma, *Appl. Catal., B*, 2014, **144**, 90.
- 20 Y. Peng, J. H. Li, L. Chen, J. H. Chen, J. Han, H. Zhang and W. Han, *Environ. Sci. Technol.*, 2012, **46**, 2864.
- 21 S. J. Yang, Y. F. Guo, H. Z. Chang, L. Ma, Y. Peng, Z. Qu, N. Q. Yan, C. Z. Wang and J. H. Li, *Appl. Catal., B*, 2013, **136**, 19.
- 22 S. Youn, S. Jeong and D. H. Kim, *Catal. Today*, 2014, **232**, 185.
- 23 R. B. Jin, Y. Liu, Z. B. Wu, H. Q. Wang and T. T. Gu, *Chemosphere*, 2010, **78**, 1160.
- 24 K. J. Lee, M. S. Maqbool, P. A. Kumar, K. H. Song and H. P. Ha, *Catal. Lett.*, 2013, **143**, 988.
- 25 R. Gao, D. Zhang, X. Liu, L. Shi, P. Maitarad, H. Li, J. Zhang and W. Cao, *Catal. Sci. Technol.*, 2013, **3**, 191.
- 26 L. Zhang, J. Pierce, V. L. Leung, D. Wang and W. S. Epling, *J. Phys. Chem. C*, 2013, **117**, 8282.
- 27 K. J. Lee, P. A. Kumar, M. S. Maqbool, K. N. Rao, K. H. Song and H. P. Ha, *Appl. Catal., B*, 2013, **142**, 705.
- 28 K. I. Hadjiivanov, *Catal. Rev.: Sci. Eng.*, 2000, **42**, 71.
- 29 C. Liu, L. Chen, J. Li, L. Ma, H. Arandiyani, Y. Du, J. Xu and J. Hao, *Environ. Sci. Technol.*, 2012, **46**, 6182.
- 30 Z. Si, D. Weng, X. Wu, Z. Ma, J. Ma and R. Ran, *Catal. Today*, 2013, **201**, 122.
- 31 R. Raj, M. P. Harold and V. Balakotaiah, *Ind. Eng. Chem. Res.*, 2013, **52**, 15455.